Article

Stabilizing Bicontinuous Nanophase Segregation in #CP#C Donor#Acceptor Blends

Zhongyuan Zhou, Xiwen Chen, and Steven Holdcroft

J. Am. Chem. Soc., **2008**, 130 (35), 11711-11718 • DOI: 10.1021/ja802021z • Publication Date (Web): 06 August 2008

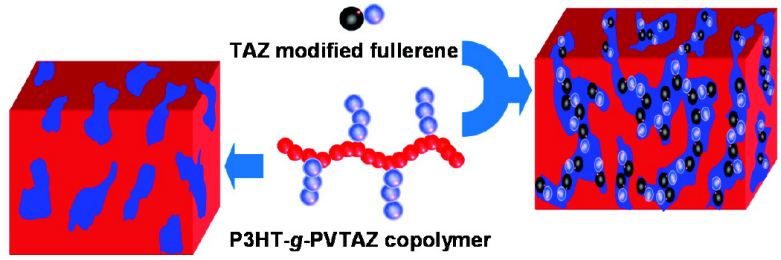

More About This Article

Additional resources and features associated with this article are available within the HTML version:

- Supporting Information
- Access to high resolution figures
- Links to articles and content related to this article
- Copyright permission to reproduce figures and/or text from this article

View the Full Text HTML

J|A|C|S
ARTICLES

Published on Web 08/06/2008

Stabilizing Bicontinuous Nanophase Segregation in πCP−C_{60} Donor−Acceptor Blends

Zhongyuan Zhou, Xiwen Chen, and Steven Holdcroft*

Department of Chemistry, Simon Fraser University, 8888 University Drive, Burnaby, BC, V5A 1S6, Canada

Received March 19, 2008; E-mail: holdcrof@sfu.ca

Abstract: The synthesis and thin film properties of a conjugated polymer bearing graft chains that are compatible with a fullerene, chemically modified with a similar motif, are described. The graft copolymer, obtained by nitroxide-mediated radical polymerization of a vinyl triazole onto a postfunctionalized poly(3-hexylthiophene) (P3HT) backbone, is blended with a fullerene modified with a pendant triazole functionality ($TAZC_{60}$). For a given ratio of polymer:$TAZC_{60}$, graft copolymer (P3HT-*g*-PVTAZ:$TAZC_{60}$) blends exhibit substantially reduced photoluminescence compared to P3HT:$TAZC_{60}$ blends, while TEM analysis reveals the graft polymer undergoes extensive mixing with the fullerene to form bicontinuous 10 nm phase domains. Graft polymer blends annealed for 1 h at 140 °C retain their nanometer phase separation as evidenced by TEM, UV−vis, XRD, and photoluminescence analysis, and phase purity was enhanced. In contrast, P3HT:$TAZC_{60}$ blends exhibit micron-sized phase-segregated morphologies before and after annealing. The chemical similarity of the triazole functionality attached to P3HT and the fullerene leads to the formation of films with uniform, stable, nanophase morphologies. This strategy may prove a useful strategy for controlling the extent of phase segregation in electron donor and acceptor blends of π-conjugated polymers (πCPs) and fullerenes.

Introduction

π-Conjugated polymers (πCPs) are currently under investigation as active materials in photovoltaic devices.[1−3] The mechanism of energy conversion involves the absorption of photons, diffusion of excitons, dissociation of excitons into positive and negative charges, and migration and capture of the charges at electrodes.[4] Since the exciton diffusion length in conjugated polymers is typically measured in the tens of nanometers, the donor/acceptor (D/A) system must be designed so that the exciton reaches the D/A interface within this length scale.[5,6] The conversion efficiency of polymer photovoltaic cells is thus strongly related to the length scale of phase segregation between donor and acceptor domains. The development of bulk D/A heterojunction structures, possessing interpenetrating, bicontinuous networks, has been found to be a potential strategy for maximizing the conversion of photons to charges while facilitating charge carrier transport through acceptor and donor domains.[7−9] Electron-donating polymers, such as poly(3-hexylthiophene) (P3HT) and poly[2-methoxy-5-(2′-ethyl-hexyloxy)-1,4-phenylene vinylene] (MEH-PPV), have been widely used as hole carriers in conjunction with soluble fullerenes, such as [6,6]-phenyl-C_{61}-butyric acid methyl ester (PCBM), which serve as the electron acceptor and electron transporting material.

Increasing the purity of the phase domains of electron donors and acceptors should provide an advantage in that the electron acceptor molecules are not isolated in the donor, and vice versa, which may circumvent charge trapping and improve device performances.[10] Various methods have been developed to optimize phase segregation. For example, Forrest et al. used organic vapor-phase deposition (OVPD) to control the consecutive crystalline growth of donor and acceptor layers.[11] Control of the extent of crystallization and morphology resulted in a low resistance, ordered, interdigitated interfaces that significantly improved solar cell efficiency. Holdcroft and co-workers developed a technique using π-conjugated polymers bearing a thermally cleavable solubilizing group to obtain pure, nanostructured phase domains of donors and acceptors.[12] Thermal annealing[13,14] or solvent annealing[15] of P3HT-PCBM produces

(1) de Gans, B. J.; Duineveld, P. C.; Schubert, U. S. *Adv. Mater.* **2004**, *16*, 203–213.
(2) Forrest, S. R. *Nature* **2004**, *428*, 911–918.
(3) Shaheen, S. E.; Brabec, C. J.; Sariciftci, N. S.; Padinger, F.; Fromherz, T.; Hummelen, J. C. *Appl. Phys. Lett.* **2001**, *78*, 841–843.
(4) Tang, C. W. *Appl. Phys. Lett.* **1986**, *48*, 183–185.
(5) Halls, J. J. M.; Pichler, K.; Friend, R. H.; Moratti, S. C.; Holmes, A. B. *Appl. Phys. Lett.* **1996**, *68*, 3120–3122.
(6) Theander, M.; Yartsev, A.; Zigmantas, D.; Sundstrom, V.; Mammo, W.; Andersson, M. R.; Inganas, O. *Phys. Rev. B* **2000**, *61*, 12957–12963.
(7) Halls, J. J. M.; Walsh, C. A.; Greenham, N. C.; Marseglia, E. A.; Friend, R. H.; Moratti, S. C.; Holmes, A. B. *Nature* **1995**, *376*, 498–500.
(8) Peumans, P.; Uchida, S.; Forrest, S. R. *Nature* **2003**, *425*, 158–162.
(9) Yu, G.; Gao, J.; Hummelen, J. C.; Wudl, F.; Heeger, A. J. *Science* **1995**, *270*, 1789–1791.
(10) Dittmer, J. J.; Marseglia, E. A.; Friend, R. H. *Adv. Mater.* **2000**, *12*, 1270–1274.
(11) Yang, F.; Shtein, M.; Forrest, S. R. *Nat. Mater.* **2005**, *4*, 37–41.
(12) Han, X.; Chen, X. W.; Holdcroft, S. *Adv. Mater.* **2007**, *19*, 1697–1702.
(13) Ma, W. L.; Yang, C. Y.; Gong, X.; Lee, K.; Heeger, A. J. *Adv. Funct. Mater.* **2005**, *15*, 1617–1622.
(14) Xiao, S.; Nguyen, M.; Gong, X.; Cao, Y.; Wu, H. B.; Moses, D.; Heeger, A. J. *Adv. Funct. Mater.* **2003**, *13*, 25–29.
(15) Li, G.; Yao, Y.; Yang, H.; Shrotriya, V.; Yang, G.; Yang, Y. *Adv. Funct. Mater.* **2007**, *17*, 1636–1644.

increased crystallinity of the P3HT and more distinguishable D/A phase morphologies, which results in improved solar cell performance. Recently, Heeger et al. showed that larger interconnected regions of a low band gap donor material and a bicontinuous network could be formed by the incorporation of additives.[16] Cumulatively, these studies indicate photovoltaic performance is improved for systems that improve the phase purity of the donor and acceptor phases, form a bicontinuous network, and produce relatively small D/A domains.

Due to the need to develop systems in which phase segregation of D/A domains can be controlled, the block and graft copolymer approach is attracting increasing interest because of their capability of forming self-assembled, well-ordered micro- and nanostructured morphologies.[17−19] For example, Jenekhe et al. reported the self-assembling behavior of rod-coil block conjugated copolymers and their encapsulation of fullerenes.[20,21] McCullough and co-workers reported on the self-assembly of regioregular polythiophene block copolymers and their electrical conductivities.[22] Mezzenga et al. studied self-assembly of PPV-based rod-coil block copolymers by varying the volume fraction of the blocks and the annealing temperature.[23,24] A block polymer is also reported in which one block is compatible with the surface of colloidal particles while the other block serves as a matrix for a doped conducting polymer, so that a single, continuous conducting phase is formed, providing a low percolation threshold for electric conductivity.[25] Several other groups have studied π-conjugated block copolymers in the context of forming bulk heterojunction PV devices. An early example is that reported by the Hadziioannou group of a diblock copolymer consisting of poly(*p*-phenylene vinylene) (PPV) and a nonconjugated block bearing C_{60} moieties.[26−30] More recently, copolymers combining various donor and acceptor motifs have been reported that modify the morphology of the films. For example, Frechet and co-workers reported a side chain diblock polymer possessing oligothiophene donor blocks and a C_{60} acceptor block, which enhances the stability of the film morphology as a compatiblizer.[31] Lindner et al. described a block polymer with donor and acceptor blocks that form a self-assembled nanostructure which can improve charge separation.[32] Kallitsis et al. described the synthesis of copolymers based on a polythiophene backbone and a poly(vinyl quinoline) graft chain,[33] whereas Holdcroft and co-workers described the synthesis of polythiophene onto which C_{60}-bearing side chains are grown.[34]

Scheme 1. Structures of the Graft Polymer and Affinity Fullerene Used in This Work

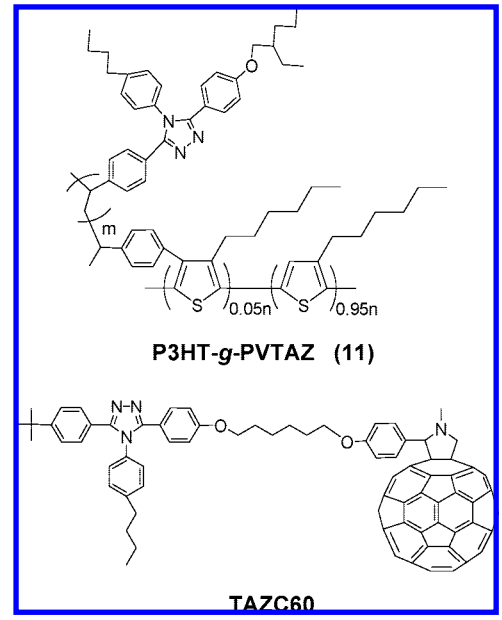

Despite these significant advances, the tailoring of π-conjugated copolymers for the purpose of controlling phase segregation is in its infancy, and systematic studies with model systems are required in order to delineate the role of the polymer structure on the morphology and to determine the role played by morphology on the properties of D/A blends. Furthermore, there is a need to investigate and develop strategies to control the ratio of donor-to-acceptor groups and to further control the size and formation of continuous nanophases that are required for charge migration and collection in PV devices.[22,28,34]

In this report, we describe a strategy for controlling the size, contiguous nature, and extent of phase segregation of donor and acceptor domains. This strategy involves the synthesis of a π-conjugated polymer bearing graft chains that are compatible with a fullerene, chemically modified with a similar motif so as to promote their intimate mixing at the nanoscopic level. This concept is demonstrated with model polymers through the synthesis of a polythiophene backbone bearing poly(vinyl triazole) graft chains and by its blending with C_{60} bearing a similar triazole moiety. The structures of the polymer and $TAZC_{60}$ are described in Scheme 1. Pendant triazole chains were chosen because they have been shown to enhance electron transport properties in OLEDs.[35−38] The synthesis and properties of C_{60} modified with a triazole group ($TAZC_{60}$) have recently

(16) Lee, J.; Ma, W. L.; Brabec, C. J.; Yuen, J.; Moon, J. S.; Kim, J. Y.; Lee, K.; Bazan, C.; Heeger, A. J. *J. Am. Chem. Soc.* **2008**, *130*, 3619–3623.
(17) Muthukumar, M.; Ober, C. K.; Thomas, E. L. *Science* **1997**, *277*, 1225–1232.
(18) Bates, F. S. *Science* **1991**, *251*, 898–905.
(19) Khandpur, A. K.; Forster, S.; Bates, F. S.; Hamley, I. W.; Ryan, A. J.; Bras, W.; Almdal, K.; Mortensen, K. *Macromolecules* **1995**, *28*, 8796–8806.
(20) Jenekhe, S. A.; Chen, X. L. *Science* **1999**, *283*, 372–375.
(21) Jenekhe, S. A.; Chen, X. L. *Science* **1998**, *279*, 1903–1907.
(22) Liu, J. S.; Sheina, E.; Kowalewski, T.; McCullough, R. D. *Angew. Chem., Int. Ed.* **2001**, *41*, 329–332.
(23) Sary, N.; Rubatat, L.; Brochon, C.; Hadziioannou, G.; Ruokolainen, J.; Mezzenga, R. *Macromolecules* **2007**, *40*, 6990–6997.
(24) Sary, N.; Mezzenga, R.; Brochon, C.; Hadziioannou, G.; Ruokolainen, J. *Macromolecules* **2007**, *40*, 3277–3286.
(25) Mezzenga, R.; Ruokolainen, J.; Fredrickson, G. H.; Kramer, E. J.; Moses, D.; Heeger, A. J.; Ikkala, O. *Science* **2003**, *299*, 1872–1874.
(26) de Boer, B.; Stalmach, U.; van Hutten, P. F.; Melzer, C.; Krasnikov, V. V.; Hadziioannou, G. *Polymer* **2001**, *42*, 9097–9109.
(27) Heiser, T.; Adamopoulos, G.; Brinkmann, M.; Giovanella, U.; Ould-Saad, S.; Brochon, C.; Van de Wetering, K.; Hadziioannou, G. *Thin Solid Films* **2006**, *511*, 219–223.
(28) Stalmach, U.; de Boer, B.; Videlot, C.; van Hutten, P. F.; Hadziioannou, G. *J. Am. Chem. Soc.* **2000**, *122*, 5464–5472.
(29) Van de Wetering, K.; Brochon, C.; Ngov, C.; Hadziioannou, G. *Macromolecules* **2006**, *39*, 4289–4297.
(30) van der Veen, M. H.; de Boer, B.; Stalmach, U.; Van de Wetering, K.; Hadziioannou, G. *Macromolecules* **2004**, *37*, 3673–3684.
(31) Sivula, K.; Ball, Z. T.; Watanabe, N.; Frechet, J. M. J. *Adv. Mater.* **2006**, *18*, 206–210.
(32) Lindner, S. M.; Huttner, S.; Chiche, A.; Thelakkat, M.; Krausch, G. *Angew. Chem., Int. Ed.* **2006**, *45*, 3364–3368.
(33) Economopoulos, S. P.; Chochos, C. L.; Gregoriou, V. G.; Kallitsis, J. K.; Barrau, S.; Hadziioannou, G. *Macromolecules* **2007**, *40*, 921–927.
(34) Chen, X. W.; Gholamkhass, B.; Han, X.; Vamvounis, G.; Holdcroft, S. *Macromol. Rapid Commun.* **2007**, *28*, 1792–1797.
(35) Kido, J.; Hongawa, K.; Okuyama, K.; Nagai, K. *Appl. Phys. Lett.* **1993**, *63*, 2627–2629.

been reported by our group.[39] It is found that $TAZC_{60}$ possesses optical and electrochemical properties that are similar to those of both C_{60} and PCBM. $TAZC_{60}$ possesses good electron transport properties, but electron mobility values are an order of magnitude lower than that of PCBM.[39] Thus, while $TAZC_{60}$ serves as an acceptable model demonstrating the use of an affinity fullerene with a π-conjugated polymer, it is not expected to yield PV devices with high photoconversion efficiencies.

The synthesis of graft polythiophenes builds on our previous contributions on postfunctionalization of P3HT, wherein partial bromination at the 4-position of the thienyl ring, followed by Pd-catalyzed coupling, enables the covalent attachment of a wide variety of functional groups.[40−42] In the present work, P3HT is functionalized with a nitroxide and is used to initiate the nitroxide-mediated radical polymerization (NMRP) of a vinyl triazole. The synthesis and polymerization of the vinyl triazole, the synthesis, characterization, and morphology of the novel graft copolymer, and the optical and morphological characterization of its blends with $TAZC_{60}$, are described.

Experimental Section

a. Chemicals. Solvents, reagents, and chemicals were purchased from Aldrich Chemical Co. and used without further purification unless otherwise stated. RR-P3HT possessing >95% regioregularity was synthesized for postfunctionalization, as described below. P3HT possessing ~92% regioregularity was purchased from Rieke Metals, Inc. (M_n = 28 000; PDI = 1.86) and was only used for preparing blends with $TAZC_{60}$. The latter was preferred as a reference material over RR-P3HT with >95% regioregularity because of its widespread use in photovoltaic applications. THF and toluene were dried over Na/benzophenone and freshly distilled prior to use. DMF was dried over barium oxide and freshly distilled prior to use.

b. Synthesis. The vinyl triazole monomer (**5**) was synthesized according Scheme 2. Synthesis and characterization of vinyl triazole monomer (**5**) and its NMRP are described in the Supporting Information.

Regioregular Poly(3-hexylthiophene) (RR-P3HT). RR-P3HT was synthesized and purified according to the method reported in literature,[43] except that Ni(dppe)Cl_2 catalyst was used instead of Ni(dppp)Cl_2. The RR-P3HT sample obtained possessed a regioregularity of >95% according to ^{1}H NMR analysis: M_n = 25 000 Da; polydispersity index = 1.7; ^{1}H NMR (δ/ppm, $CDCl_3$) 6.99 (s, 1H), 2.79 (t, 2H), 1.72 (m, 2H), 1.34 (m, 5H), 0.90 (t, 3H).

1-[4-(4′-Trimethylene-1,3,2-dioxaborolan-2-yl)phenyl]]-1-(2,2,6,6-tetramethyl-1-piperidinyloxyl)ethane (8). 8 was synthesized according to the method reported in literature.[34] ^{1}H NMR (CD_2Cl_2) δ (ppm): 0.61, 1.01, 1.16, 1.28 (each s, 12H), 1.26−1.58 (m, 6H), 1.45 (d, 3H), 2.04 (quintet, 2H), 4.13 (t, 4H), 4.76 (q, 1H), 7.29 (d, 2H), 7.66 (d, 2H).

5% BrP3HT (9). To a flask containing RR-P3HT (0.20 g, 1.20 mmol) in chloroform (14 mL) was added NBS (11.0 mg, 0.06 mmol). The solution was stirred at room temperature for 15 h and heated at 50 °C for 2 h. The reaction mixture was poured into a saturated $NaHCO_3$ solution (50 mL). The organic layer was washed with water five times and dried over $MgSO_4$. Precipitation into methanol gave a black solid (0.18 g, yield 90%). ^{1}H NMR ($CDCl_3$) δ (ppm): 2.78 (br, methylene), 2.62 (br, methylene), 1.60 (br), 1.33 (br), 1.28 (br), 0.87 (br, CH_3). GPC: M_n = 27 000 Da; PDI = 1.74.

Scheme 2. Synthetic Route for Vinyl Triazole Monomer (**5**) and the Polymerization of **5** by NMRP to PVTAZ (**6**)

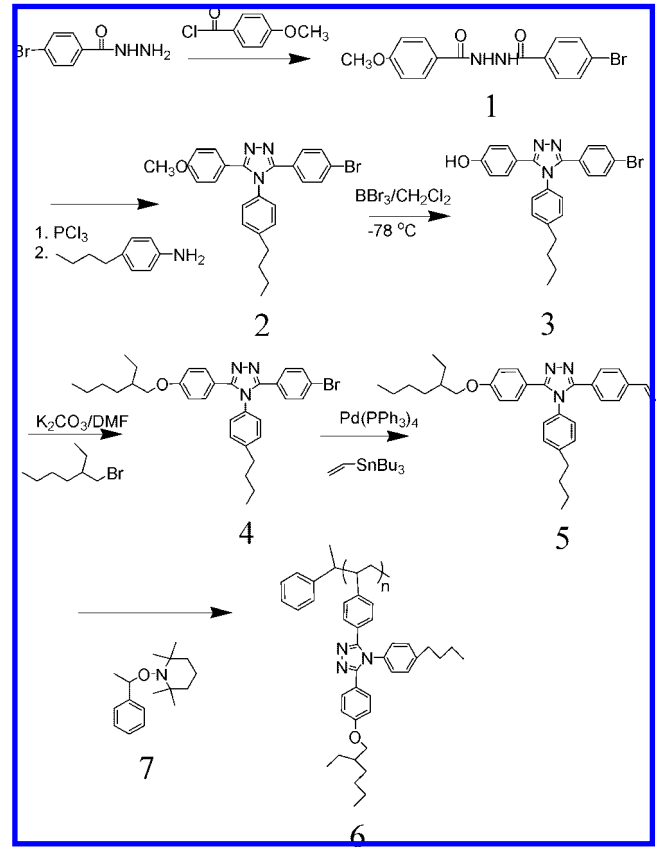

5% TEMPO-P3HT (10). 5% BrP3HT (**9**) (150 mg, 0.90 mmol) was dissolved in 15 mL of THF. **8** (0.155 g, 0.045 mmol) and 2 M Na_2CO_3 aqueous solution (0.6 mL, 1.2 mmol) were added. The mixture was deoxygenated by bubbling nitrogen for 30 min. $Pd(PPh_3)_4$ (5 mg, 0.004 mmol) was added and the flask heated at 60 °C for 3 days under nitrogen. The mixture was concentrated and precipitated into methanol. The solid was purified by Soxhlet extraction with methanol and precipitated again into methanol from a chloroform solution and dried in a vacuum oven; 120 mg of a black solid was obtained (yield 80%). ^{1}H NMR ($CDCl_3$) δ (ppm): 2.71 (br, methylene), 1.60 (br), 1.33 (br), 1.28 (br), 0.87 (br, CH_3). GPC: M_n = 31 000 Da; PDI = 1.84.

P3HT-*g*-PVTAZ (11). Macroinitiator (**10**) (100 mg, 0.60 mmol), acetic anhydride (0.4 mL), and vinyl TAZ monomer (**5**) (0.06 g, 0.12 mmol) were added to 6.5 mL of *p*-xylene. The mixture was deoxygenated by three freeze−pump−thaw cycles, maintained under argon, and placed in an oil bath at 125 °C. After 2 days at 125 °C, the mixture was cooled and solvent was dried under vacuum. The polymer purified on a silica gel column using ethyl acetate. After workup, 118 mg of brown solid was obtained. GPC: M_n = 39 200 Da; PDI = 1.85.

c. Measurements. ^{1}H NMR spectra were obtained on a 500 MHz Varian AS500 spectrometer; chemical shifts are reported in parts per million (ppm), referenced to CD_2Cl_2 (^{1}H: δ = 5.32) or $CDCl_3$ (^{1}H: δ = 7.26). Molecular weights were measured by gel permeation chromatography (GPC) (Waters model 1515 isocratic pump) equipped with μ-Styragel columns against polystyrene standards. Polymers were eluted with THF using a flow rate of 1.0 mL/min and detected with a UV−vis detector (Waters model 2487) at 254 nm. Elemental analyses were using a Carlo Erba model 1106

(36) Strukelj, M.; Miller, T. M.; Papadimitrakopoulos, F.; Son, S. *J. Am. Chem. Soc.* **1995**, *117*, 11976–11983.
(37) Strukelj, M.; Papadimitrakopoulos, F.; Miller, T. M.; Rothberg, L. J. *Science* **1995**, *267*, 1969–1972.
(38) Yu, L. S.; Chen, S. A. *Adv. Mater.* **2004**, *16*, 744–748.
(39) Chen, X. W.; Liu, C. Y.; Jen, T. H.; Chen, S. A.; Holdcroft, S. *Chem. Mater.* **2007**, *19*, 5194–5199.
(40) Li, Y. N.; Vamvounis, G.; Yu, J. F.; Holdcroft, S. *Macromolecules* **2001**, *34*, 3130–3132.
(41) Li, Y. N.; Vamvounis, G.; Holdcroft, S. *Macromolecules* **2001**, *34*, 141–143.
(42) Li, Y. N.; Vamvounis, G.; Holdcroft, S. *Macromolecules* **2002**, *35*, 6900–6906.
(43) Loewe, R. S.; Ewbank, P. C.; Liu, J. S.; Zhai, L.; McCullough, R. D. *Macromolecules* **2001**, *34*, 4324–4333.

CHN analyzer. UV−vis absorption spectra were recorded on a Cary 3EI (Varian) spectrophotometer. Polymeric films were prepared by either spin-coating 5 mg/mL THF solutions of the polymer, or spin-coating 15 mg/mL solutions of polymer and TAZC60, at 700 rpm. Photoluminescence (PL) spectra and quantum efficiency measurement were recorded with a Photon Technology International QuantumMaster model QM-4 equipped with an integrating sphere. Film thickness and surface roughness were measured using a KLA-Tencor Alpha-Step IQ Surface Profiler. Cyclic voltammetry was carried out using a potentiostat/galvanostat Model 263A from Princeton Applied Research. A one-compartment, three-electrode cell was used with a glassy carbon disk coated with polymer and Pt wires as working and counter electrodes, respectively. The reference electrode consisted of a Pt wire in an acetonitrile solution of 0.1 M Bu_4NI/0.05 M I_2, which was separated from the working electrode compartment by a glass frit. The electrolyte was a solution of 0.1 M Bu_4NClO_4 in dry acetonitrile deoxygenated by bubbling with nitrogen. The potential scan rate was 50 mV/s. Ferrocene was added to the electrolyte after the voltammetry of the polymers and served as an internal standard for calibrating the potential of the reference electrode. Transmission electron microscope (TEM) images were performed on a Hitachi H7600 TEM or Tecnai 20 FEI STEM. A layer of poly(styrene sulfonic acid)-doped poly(3,4-ethylenedioxythiophene) (PEDOT, BaytonP VP AI4083) was spin cast on cleaned glasses at 5000 rpm and annealed at 140 °C for 10 min. Onto this surface, polymers and polymer blends were spin cast and films dried in air. The film and substrate were immersed into water and the polymer films picked up with Cu grids from the surface of the water. All the films on Cu grids were stained for 15 min using RuO_4 vapor prepared in situ with 0.5% ruthenium(III) chloride in a sodium hypochlorite solution. X-ray diffractometry was performed on a Bruker-AXS D8 Discover high-resolution diffractometer system using Cu Kα wavelength (about 1.544 Å). Polymer films were prepared on silicon wafer substrates by spin casting.

Results and Discussion

Polymer Synthesis. The vinyl triazole monomer (**5**) was synthesized according Scheme 2. Following condensation of 4-bromobenzoyl hydrazine and *p*-anisoyl chloride, 1-(*p*-anisoyl) 2-(4′-bromo)benzoyl hydrazide (**1**) was formed as evidenced by the two hydrazide proton peaks at 10.4 and 10.6 ppm in the ^{1}H NMR spectrum of **1**. Other NMR peaks due to **1** are observed at 7.0−8.0 (aryl, 8H), and 3.8 ppm (anisoyl, 3H). **1** was reacted with 4-*n*-butylaniline to form 3-(4′-anisoyl)-4-(4′-*n*-butylphenyl)-5-(4′-bromophenyl)-1,2,4-triazole (**2**). The ^{1}H NMR spectrum indicates that the two peaks at 10.4 and 10.6 ppm due to hydrazide had disappeared. **2** possessed peaks at 6.8−7.5 (aryl, 12H), 2.7, 1.7, 1.4 (methylene, 6H), 3.8 (anisoyl, 3H), and 0.9 ppm (methyl, 3H). In order to enhance the solubility of the triazole compound, the anisoyl group was converted to a hydroxide group to form 3-(4′-phenoyl)-4-(4′-*n*-butylphenyl)-5-(4′-bromophenyl)-1,2,4-trizole (**3**), which was confirmed by the disappearance of the ^{1}H NMR peak at 3.8 ppm due to anisoyl, and the emergence of a peak at 9.95 ppm due to the hydroxide group. The ethylhexyl group was attached using the Williamson reaction to form 3-(4′-(2″-ethylhexyloxy)phenyl)-4-(4′-*n*-butylphenyl)-5-(4′-bromophenyl)-1,2,4-triazole (**4**). The ^{1}H NMR spectrum of **4** indicated that the hydroxide peak at 9.95 ppm was absent, and peaks due to $-OCH_2-$ (3.70 ppm) and the ethylhexyl group (0.9−1.8 ppm, 15H) were present. A Heck coupling of vinyltributyltin to **4** afforded the vinyl triazole monomer, 3-(4′-(2″-ethylhexyloxy)phenyl)-4-4′-*n*-butylphenyl)-5-(4′-vinylphenyl)-1,2,4-triazole (**5**). The ^{1}H NMR spectrum of **5** revealed three peaks due to the vinyl group at 6.70, 5.78, and 5.29 ppm, in addition the peaks due to the triazole moiety.

Scheme 3. Synthetic Route for Graft Copolymer (**11**)

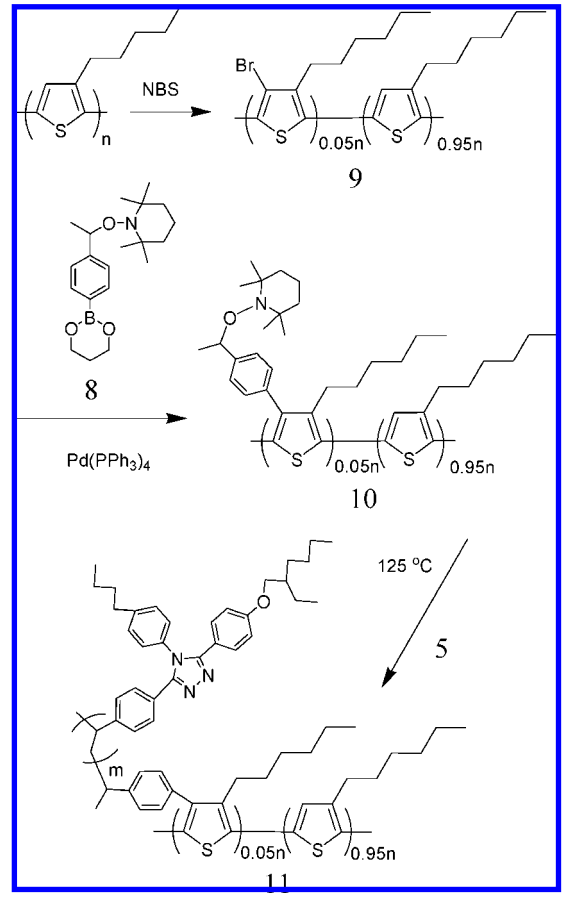

Since **5** is a monomer prepared for the first time, intended to be polymerized onto RR-P3HT by NMRP, a demonstration of its NMRP of **5** was warranted. The polymerization of **5** to its polymer (**6**) was initiated by a TEMPO compound (**7**). The evolution of the GPC traces of **6** is shown in Supporting Information, Figure S1a, as is a plot of the molecular weight versus polymerization time (Figure S1b). The molecular weight of **6** increased linearly with reaction time, and the polymers possessed a polydispersity index between 1.05 and 1.15, indicating typical pseudo-controlled, radical polymerization behavior. The synthetic scheme for the graft copolymer **11** is shown in Scheme 3. The aim was to substitute only 5% of the 4-thienyl protons with a graft chain since previous studies[42] have shown that much larger degrees of substitution with bulky functional groups disrupt the coplanarity of the π-conjugated backbone leading to reduced polycrystallinity of the P3HT—resulting in a large shift in the absorption spectrum and, potentially, reduced hole conductivity. However, Frechet and co-workers recently reported the surprising result that P3HT containing 4% of the 3,4-dihexyl derivative confers improved thermal stability of solar cell devices due to increased stabilization of the morphology.[44] For similar reasons of promoting organized structures with the highest hole mobilities and lowest energy absorption spectra possible, regioregular RR-P3HT was used as the starting material. The ^{1}H NMR spectrum of the poly(3-hexylthiophene) (RR-P3HT) prepared indicated that the regioregularity was >95% (see Supporting Information, Figure S2). The spectrum shows peaks corresponding to α-methylene

(44) Sivula, K.; Luscombe, C. K.; Thompson, B. C.; Frechet, J. M. J. *J. Am. Chem. Soc.* **2006**, *128*, 13988–13989.

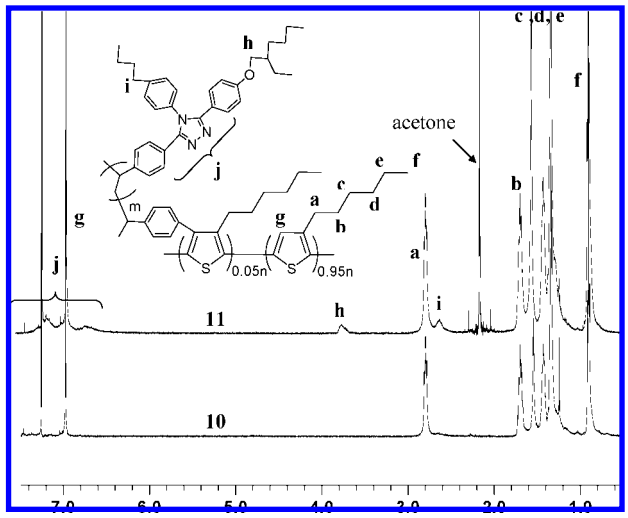

Figure 1. ^{1}H NMR spectra of macroinitiator (**10**) and the resulting graft copolymer P3HT-*g*-PVTAZ (**11**).

protons at 2.78 ppm, which are indicative of hexyl chains on adjacent thienyl units linked head-to-tail; only a very small peak is observed at 2.58 ppm, which is attributed to head-to-head linkages. RR-P3HT was brominated at the 4-position via electrophilic substitution to 5 mol % (based on the thienyl ring). The α-methylene protons, for which bromine is located on the same thienyl ring, are observed at 2.62 ppm (see Supporting Information, Figure S3). Integration of the α-methylene protons' peak at 2.62 ppm indicated that 5% of the RR-P3HT backbone was brominated.

Partially brominated P3HT (**9**) was used in the Suzuki cross-coupling reaction with a boronic ester of a nitroxide to form the macroinitiator (**10**), comprising a polythiophene bearing a TEMPO group on the thienyl ring, following the reported method for full postfunctionalization of P3HT.[34] Previous studies of 100% postfunctionalization of P3HT backbone with various functional groups indicate a phenyl ring attached to the 4-position of an alkyl-substituted thiophene shifts the α-methylene peak from 2.78 to 2.26 ppm.[26] The peak at 2.26 ppm in the ^{1}H NMR spectrum of **10** (see Supporting Information, Figure S4, inset) is thus assigned to α-methylene protons associated with a thienyl ring bearing a TEMPO group. By integrating the peak at 2.26 ppm, it is found that 5 mol % of the RR-P3HT backbone was functionalized; that is, conversion of the bromo to nitroxide group is quantitative. The macroinitiator (**10**) was used to initiate the NMRP of **5**, so as to grow poly(vinyl triazole) from the conjugated polymer backbone. The polymerization was carried out at 125 °C under argon. A graft copolymer, **11**, was synthesized using a monomer:initiator ratio of 5. Gel permeation chromatograms of the macroinitiator (**10**) and the graft polymers (**11**) are shown in Figure S5 of the Supporting Information. Each possessed single and narrow molecular weight distributions. GPC analysis, using THF as eluent and polystyrene calibration standards, indicates that M_n for **10** and **11** are 31 000 (PDI = 1.84) and 39 200 (PDI = 1.85) Da, respectively.

The ^{1}H NMR spectra of **11** are shown in Figure 1. The spectrum reveals protons associated with the P3HT backbone and PVTAZ side chain. Of note, the peaks due to α-methylenes and aromatic protons of the P3HT backbone appear at 2.78 (m, 2H) and 6.98 ppm (s, 1H), respectively. **11** possesses signature peaks at 6.7−7.3 (aryl, 12H), 3.70 (−OCH_2−, 2H), and 2.63 ppm (α-methylene, 2H). Protons at 5.78 and 5.29 ppm, due to the vinyl group, and previously observed for **5**, are notably

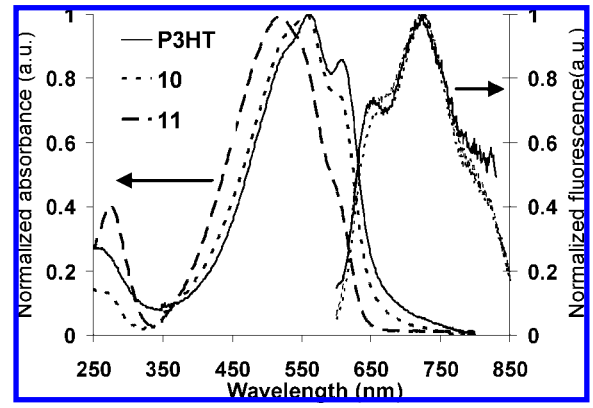

Figure 2. UV−vis and PL spectra of RR-P3HT, **10**, and **11** films spin cast from THF solutions.

absent. The molar ratio of thienyl units to TAZ groups calculated from the integrals of the peaks at 2.78 ppm (α-methylene of 3-hexylthienyl and 3.70 ppm (−OCH_2−, TAZ group) was 6:1. Given that the α-methylene and −OCH_2− integrals possess two protons per group, and as 5 mol % of the thienyl units bear graft chains, the average degree of polymerization of **5** onto the main chain was 3.3 (3). Thus the side chain is an oligomer rather than a polymer, but for the purpose of grammatical consistency, the term polymer is used throughout.

Optical Properties. Normalized UV−vis spectra of RR-P3HT, **10**, and **11** in solution possess almost identical absorption spectra (λ_{max} 445 nm) (see Supporting Information, Figure S6). Thus the electronic structures of isolated π-conjugated polymer chains in solution are unperturbed by the presence of the short PVTAZ side chain. Similarly, the PL spectra of RR-P3HT, **10**, and **11** exhibit identical emission maxima (λ_{max} 572 nm) (see Supporting Information, Figure S7), indicating that the PVTAZ side chains do not perturb the excited-state structure of π-conjugated polymer chains in solution relative to ∼95% rr P3HT. In contrast, subtle differences are observed in the solid state spectra. As observed in Figure 2, the absorption due to the triazole in **11** occurs at 278 nm. The absorption maximum of **11** due to the $\pi-\pi^*$ transition is blue-shifted 35 nm compared to both RR-P3HT and **10**, and the vibronic splitting, observed as the shoulder at 603 nm, diminishes in the order RR-P3HT > **10** > **11**, indicating a decreasing degree of ordering in the solid state. The photoluminescence of films of RR-P3HT, **10**, and **11** (see Figure 2) showed very similar maximum emission wavelengths, 728 nm, indicating that the graft side chain does not perturb the electronic structure of the emitting exciton associated with the main chain. The quantum yields of fluorescence, Φ_{fl}, for films of RR-P3HT, **10**, and **11** are 0.020, 0.023, and 0.051, respectively. The value for RR-P3HT is typical,[26] and the value for **11** is consistent for functionalized P3HTs, which exhibit higher fluorescence efficiency because the 4-functionality increases the distance between stacks of chains, thereby reducing self-quenching.[42]

Redox Properties. CVs of RR-P3HT, **10**, and **11** are shown in Figure 3, from which HOMO and LUMO energy levels can be approximated by considering the onset potential of oxidation and reduction. Redox energy levels were measured against the Fc/Fc^+ redox couple, which is 4.8 eV with respect to an electron in vacuo.[45] The onset of oxidation for RR-P3HT, **10**, and **11**

(45) Pommerehne, J.; Vestweber, H.; Guss, W.; Mahrt, R. F.; Bassler, H.; Porsch, M.; Daub, J. *Adv. Mater.* **1995**, *7*, 551–554.

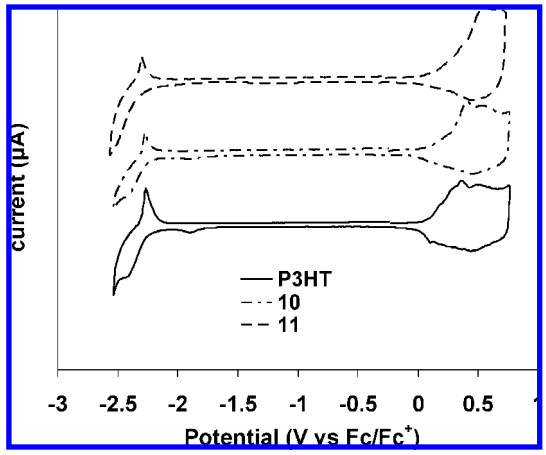

Figure 3. Cyclic voltammograms of films of RR-P3HT, **10**, and **11**.

are +0.08 V vs Fc/Fc^+, indicating a HOMO level of ~4.9 eV. Furthermore, a clear n-doping process with an onset potential at −2.24 V is observed that is reversible. This indicates the polymers exhibit both p-type and n-type behavior, which is consistent with the observation, from studies of field effect transistors, that these polymers are ambipolar.[46] The electron affinities for the three polymers are estimated to be ~2.6 eV. The presence of the TEMPO or PVTAZ graft chain thus has no visible influence on the redox properties of the main chain.

Morphology of Thin Films and of Its Blends with $TAZC_{60}$. **11** was designed in order to investigate the role of the graft chain on the formation of blends with $TAZC_{60}$. The morphologies of the graft copolymers and its blends with $TAZC_{60}$ were studied by TEM. The staining agent, RuO_4, preferentially oxidizes P3HT domains (oxidation potential ~ 4.9 eV) rather than TAZ domains (oxidation potential ~ 6.3 eV) or $TAZC_{60}$ domains (oxidation potential ~ 5.9 eV),[39] producing highly scattering RuO_2.[47,48] The dark regions of the TEM images therefore represent P3HT domains; the lighter regions, PVTAZ (side chain) or $TAZC_{60}$ domains. Films of **11** and **11**:$TAZC_{60}$ blends consisting of 1:1 and 1:2 weight ratios were prepared. Micrographs are shown in Figure 4a−c and reveal that films of **11**, and its blends, possess uniform, phase-segregated morphologies. They also reveal that the lighter regions in micrographs of **11** grow in relative size with increasing $TAZC_{60}$ content, providing evidence that $TAZC_{60}$, with its polar TAZ functionality (similar to the graft structure of **11**), mixes with the PVTAZ domains associated with **11**. As a control experiment, unmodified P3HT (~92% regioregularity) was blended with $TAZC_{60}$ and the morphology examined. All attempts to form uniform, miscible films of P3HT and $TAZC_{60}$ failed—as exemplified by the TEM of the 1:1 weight blend shown in Figure 4d, which shows large-scale (micron-sized) phase separation of P3HT-rich phase surrounded by $TAZC_{60}$-rich phase. Furthermore, the average surface roughness of blends of **11**, determined by surface profilometry, was <2 nm, while for blends of P3HT and $TAZC_{60}$, the roughness was >18 nm.

The UV−vis absorption spectra of films of P3HT:$TAZC_{60}$ and **11**:$TAZC_{60}$ blends were similar. The concomitant change in UV−vis absorption spectra of **11** and P3HT with increasing $TAZC_{60}$ content is shown in Figure 5a,b. With increasing $TAZC_{60}$ content, the extinction coefficient of the polymer blends (**11**:$TAZC_{60}$ and P3HT:$TAZC_{60}$) decreases, λ_{max} blue shifts, and

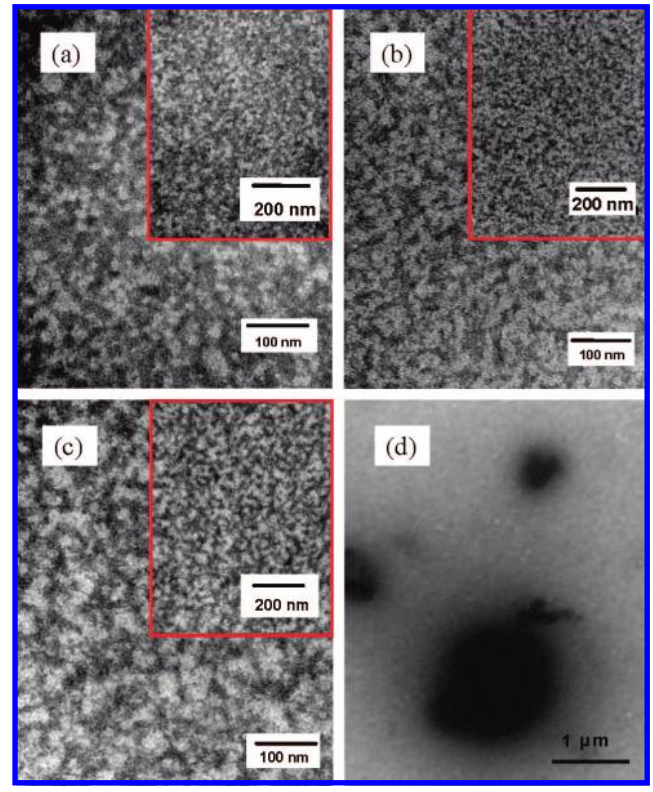

Figure 4. TEM of (a) **11**, (b) **11**:$TAZC_{60}$ (1:1 wt % blend), (c) **11**:$TAZC_{60}$ (1:2 wt % blend), (d) P3HT:$TAZC_{60}$ (1:1 wt % blend). Inset images are lower magnification.

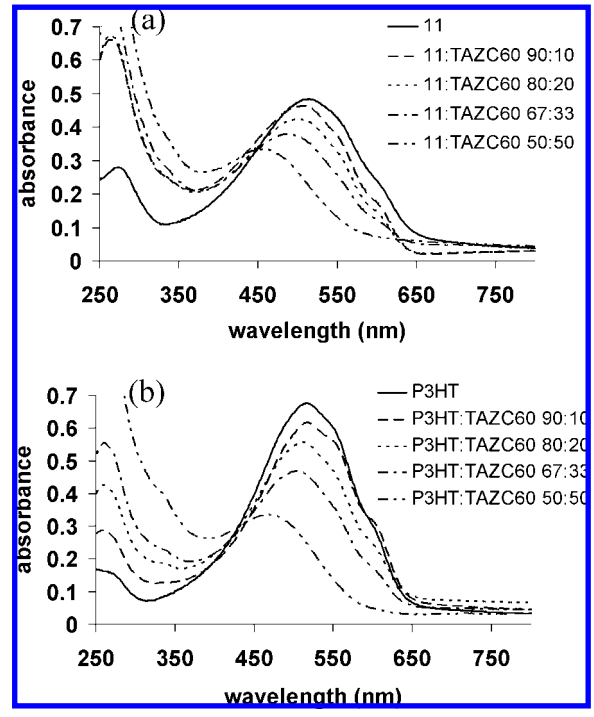

Figure 5. UV−vis absorption spectra of films spin cast from (a) **11** and (b) P3HT in chlorobenzene solutions containing various weight ratios of $TAZC_{60}$.

(46) Chua, L. L.; Zaumseil, J.; Chang, J. F.; Ou, E. C. W.; Ho, P. K. H.; Sirringhaus, H.; Friend, R. H. *Nature* **2005**, *434*, 194–199.
(47) Trent, J. S.; Scheinbeim, J. I.; Couchman, P. R. *Macromolecules* **1983**, *16*, 589–598.
(48) Hong, S.; Bushelman, A. A.; MacKnight, W. J.; Gido, S. P.; Lohse, D. J.; Fetters, L. J. *Polymer* **2001**, *42*, 5909–5914.

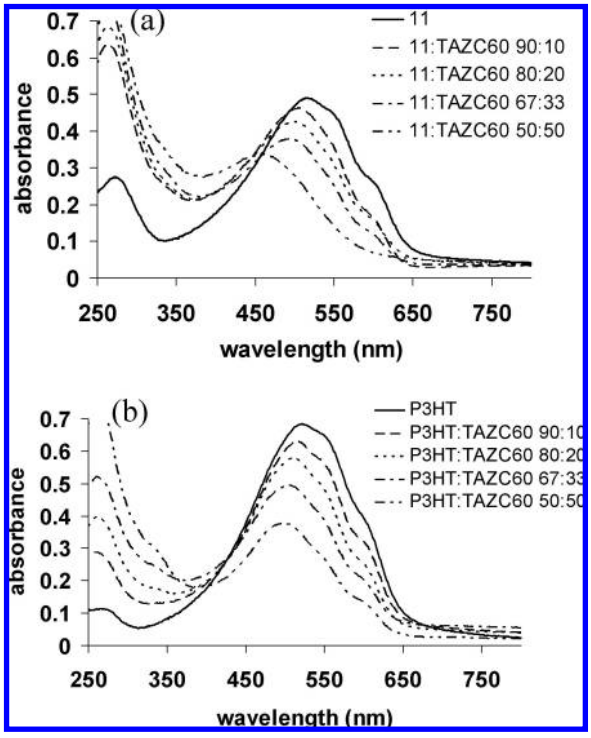

Figure 6. UV−vis absorption spectra of films after annealing at 140 °C for 1 h (a) **11** and (b) P3HT containing various weight ratios of $TAZC_{60}$.

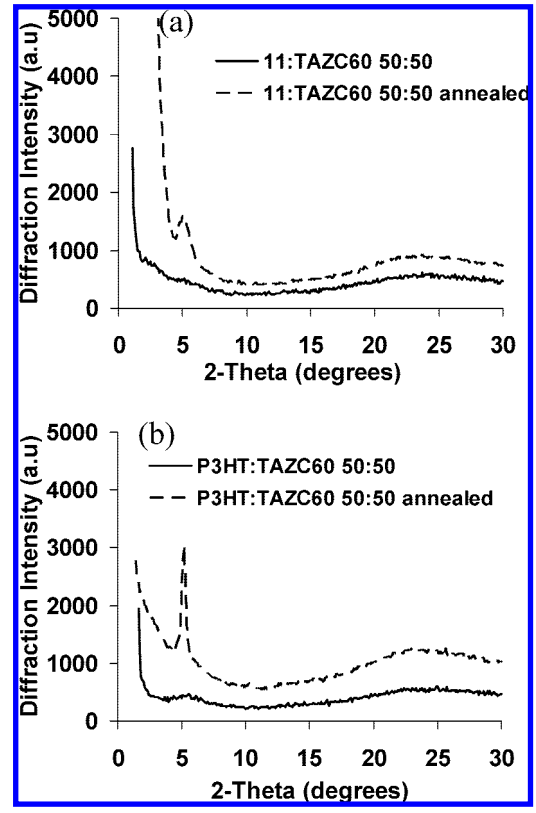

Figure 7. XRD spectra of blended films before and after annealing at 140 °C for 1 h: (a) **11**:$TAZC_{60}$, (b) P3HT:$TAZC_{60}$.

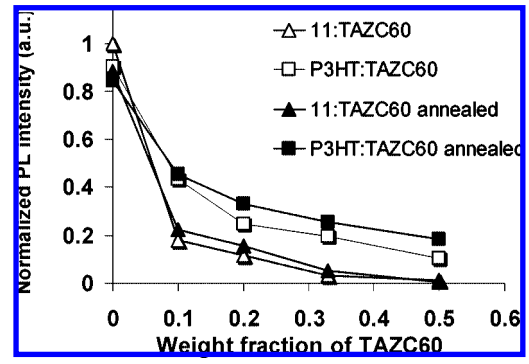

Figure 8. Photoluminescence intensity normalized to absorbance at 480 nm.

the vibronic features are less observable. This indicates that intermolecular interchain interactions of the π-conjugated system are weakened with increasing $TAZC_{60}$ content in the blends.

The glass transition temperature of P3HT is 125 °C.[1] The annealing temperature is usually 10 °C higher than T_g of the materials.[49] Sivula et al.[31] reported a macrosize phase morphology of a P3HT-PCBM blend film that was annealed at 140 °C for 1 h. We also used 140 °C for 1 h to anneal polymer blends. The λ_{max} of **P3HT**:$TAZC_{60}$ blends subsequently red-shifted; for example, λ_{max} for a 50:50 blend ratio shifted from 464 to 497 nm, and the vibronic features increased in intensity as shown in Figure 6. In contrast, annealing blends of **11**:$TAZC_{60}$ did not produce any noticeable change in the UV−vis spectra. XRD of annealed 50:50 blends of **11**:$TAZC_{60}$ and P3HT:$TAZC_{60}$ blends (see Figure 7) revealed an increase in intensity of the peak at $2\theta \approx 5°$ (corresponding to the interchain spacing in P3HT associated with the interdigitated alkyl chains).[50] The intensity of the XRD peak for the P3HT:$TAZC_{60}$ blend is much stronger than that for the **11**:$TAZC_{60}$ blend, which indicates much more extensive organization and self-assembly of the P3HT in the former.

PL spectra for films of **11**:$TAZC_{60}$ and P3HT:$TAZC_{60}$ prior to thermal annealing are shown in the Supporting Information (Figure S8a,b; the corresponding decreases in PL intensity plotted against composition for the two systems is shown in Figure 8). Both systems are characterized as exhibiting decreasing PL intensity with increasing $TAZC_{60}$ content due to photoinduced electron transfer,[51] but PL quenching is considerably greater for the **11**:$TAZC_{60}$ systems. For example, in the 90:10 blend of **11**:$TAZC_{60}$, the PL intensity is only 18% of **11**; whereas for P3HT:$TAZC_{60}$ with the same composition, PL is 50% of pure P3HT. Similarly, for a 50:50 blend, emission from **11** is completely quenched, whereas the P3HT blend maintains 12% of its original PL intensity. After annealing at 140 °C for 1 h, as shown in the Supporting Information (Figure S9a,b), both PL of copolymer **11** and P3HT decreased because annealing induces stronger interchain−interlayer interactions of the P3HT chain;[52] however, as shown in Figure 8, the PL intensity increases for P3HT:$TAZC_{60}$ blends after annealing, while for blends of **11**:$TAZC_{60}$, the increase in PL with annealing was much smaller for 90:10, 80:20, and 67:33 weight blends and PL remained completely quenched for 50:50 blends. This, again, showed, after annealing P3HT:$TAZC_{60}$ blends, the

(49) Mihailetchi, V. D.; Xie, H. X.; de Boer, B.; Koster, L. J. A.; Blom, P. W. M. *Adv. Funct. Mater.* **2006**, *16*, 699–708.
(50) Chen, T. A.; Wu, X. M.; Rieke, R. D. *J. Am. Chem. Soc.* **1995**, *117*, 233–244.
(51) Sariciftci, N. S.; Smilowitz, L.; Heeger, A. J.; Wudl, F. *Science* **1992**, *258*, 1474–1476.
(52) Cornil, J.; Beljonne, D.; Calbert, J. P.; Bredas, J. L. *Adv. Mater.* **2001**, *13*, 1053–1067.

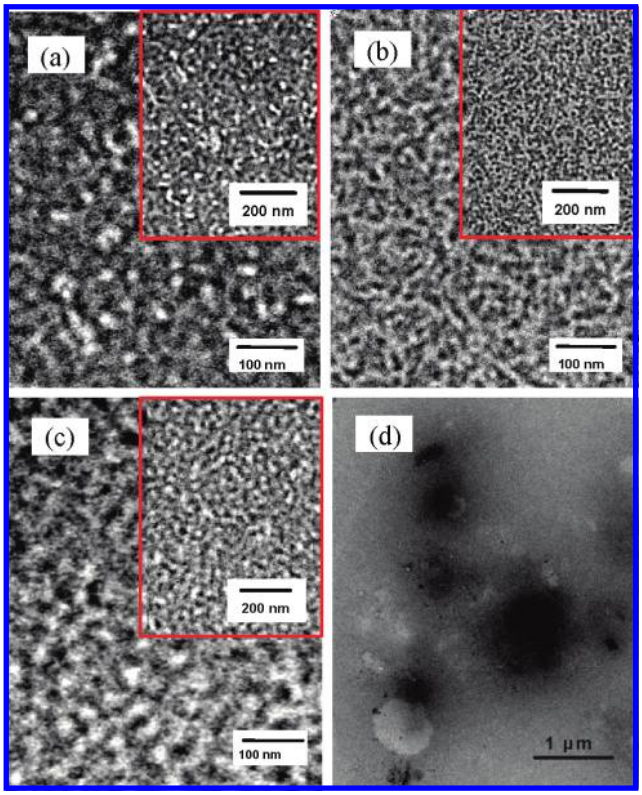

Figure 9. Transmission electron micrographs for films after annealing at 140 °C for 1 h: (a) **11**, (b) **11**:$TAZC_{60}$ (1:1 wt %), (c) **11**:$TAZC_{60}$ (1:2 wt %), (d) P3HT:$TAZC_{60}$ (1:1 wt %). Inset images are lower magnification.

P3HT showed substantial reorganization, whereas blends of **11**:$TAZC_{60}$ were morphologically stable. These data suggest that, in the case of P3HT:$TAZC_{60}$ films, mixing of $TAZC_{60}$ with P3HT occurs to some degree (despite TEMs of solution cast films indicating large-scale phase separation), thereby lowering PL by photoinduced electron transfer; and that upon annealing, the $TAZC_{60}$ is expelled from the P3HT domains, which increase in molecular order (see XRD data) yet become more fluorescent. The latter can only be explained by a reduction in the rate of photoinduced electron transfer from P3HT to $TAZC_{60}$ as a result of the phase domains of P3HT and $TAZC_{60}$ becoming larger, and more distant from each other, since an increased molecular order of P3HT is normally accompanied by a reduction in PL intensity. In contrast, PL intensities in films of **11**:$TAZC_{60}$ remain constant, and low, after annealing, which suggests the domains remain much more stabilized.

TEM morphologies of polymers **11** and its blends with $TAZC_{60}$, after annealing, are shown in Figure 9. After annealing, the contrast becomes stronger; dark regions (P3HT), in general, appear darker; light regions (TAZ), lighter. The morphology of blends of the **11**:$TAZC_{60}$ becomes more distinguishable, although the phase domains remain ~10 nm in size, indicating both improved phase purity and stabilized nanophase segregation. In contrast to **11**:$TAZC_{60}$ blends, P3HT:$TAZC_{60}$ blends maintained large-scale phase separation after annealing. Further annealing at 150 °C for 3 h did not result in any subsequent change in morphology.

Conclusion

In summary, this work describes the synthesis of a triazole monomer (**5**) and its NMRP, the synthesis of a macroinitiator (**10**) consisting of a polythiophene backbone bearing nitroxide groups, the synthesis of a graft copolymer consisting of a polythiophene backbone bearing polyvinyl triazole moieties (**11**), and the preparation of blends of a graft copolymer with a fullerene possessing a chemically similar motif ($TAZC_{60}$). **11** possesses similar optical and electrochemical properties to P3HT (~92% regioregular), the latter being a preferred polymer for study in photovoltaic devices, but it is found that the miscibility of the blend with $TAZC_{60}$ is substantially different. **11** forms a bicontinous phase of πCP and triazole. The latter is compatible with fullerene modified with a pendant triazole moiety, and **11**:$TAZC_{60}$ blends form interconnected phase domains 10 nm in size by virtue of the attachment of TAZ groups to polymer, as demonstrated by TEM, UV−vis, PL quenching, and XRD measurements. P3HT, in contrast, is not miscible with $TAZC_{60}$ and phase separates into microsized domains.

While the incorporation of short oligomer side chains onto regioregular P3HT facilitates the formation of a bicontinuous nanonetwork, it is noted that the result is that the P3HT component of **11** adopts a degree of twisting (noncoplanarity) when blended with $TAZC_{60}$, as evidenced by the blue shift in the absorption spectrum and the absence of strong XRD patterns. P3HT in P3HT:$TAZC_{60}$ blends also adopts a degree of noncoplanarity, but annealing the P3HT:$TAZC_{60}$ blends enables the P3HT to adopt a more organized, semicrystalline structure. In contrast, annealing blends of **11**:$TAZC_{60}$ do not produce a more organized, semicrystalline P3HT component. The conclusion of this work therefore is three-fold: the incorporation of oligomeric side chains onto regioregular P3HT facilitates the formation of a bicontinuous nanoscale network; the morphology of the of the πCP in blends of the **11**:$TAZC_{60}$ is stabilized; but the P3HT component is not able to adopt a highly organized, semicrystalline structure. The latter may potentially be mitigated by manipulating the microstructure of the polymer through the sequence length distribution of grafts along the main chain (graft density) and the length of the side chains (graft length), in a manner previously shown for proton conducting graft copolymers.[53] The results of this work are intended to stimulate further examination of the role of molecular architecture of π-conjugated polymers on the evolution of controlled nanosegregated, donor−acceptor morphologies.

Acknowledgment. We thank the Natural Sciences and Engineering Research Council of Canada for financial support.

Supporting Information Available: Synthesis of compounds **1**−**7**, GPC curves and molecular weight versus reaction time for NMRP of monomer **5**, ^{1}H NMR spectra of RR-P3HT and polymers **9**−**11**, GPC curves of polymers **10** and **11**, UV−vis absorption and PL spectra of RR-P3HT, **10**, and **11** in THF solutions, and PL spectra of **11**:$TAZC_{60}$ and P3HT:$TAZC_{60}$ blend films. This material is available free of charge via the Internet at http://pubs.acs.org.

JA802021Z

(53) Ding, J. F.; Chuy, C.; Holdcroft, S. *Adv. Funct. Mater.* **2002**, *12*, 389–394.